OPEN ACCESS

GAVIN PUBLISHERS

Biosensors and Bioelectronics Open Access

Research Article

Chen L, et al. Biosens Bioelectron Open Acc: BBOA-145.

DOI: 10.29011/ 2577-2260. 100045

Cell Manipulation and Detection Enhancement Enabled by a Microelectromagnet Integrated with a Digital Microfluidic Device

Liji Chen, Andrew C. Madison, Richard B. Fair*

Department of Electrical and Computer Engineering, Duke University, Durham, NC, USA

***Corresponding author:** Richard B. Fair, Department of Electrical and Computer Engineering, Duke University, Durham, NC, USA. Tel: +1-9196605277; Email: rfair@duke.edu

Citation: Chen L, Madison AC, Fair RB (2018) Cell Manipulation and Detection Enhancement Enabled by a Microelectromagnet Integrated with a Digital Microfluidic Device. Biosens Bioelectron Open Acc: BBOA-145. DOI: 10.29011/ 2577-2260. 100045

Received Date: 26 September, 2018; **Accepted Date:** 25 October, 2018; **Published Date:** 01 November, 2018

Abstract

This work demonstrates sparse cell detection in mL samples, using magnetic bead manipulation on an Electrowetting-On-Dielectric (EWD) chip. Sparse sample detection was performed in two steps: cell capture off chip from the starting solution with a microelectromagnet and on-chip fluorescent signal detection on an EWD chip. In the first step, immunological reactions enable the binding between target cells and antibody-coated magnetic beads, which enabled sample capture with high cell survival rates. In the second step, fluorescent detection is achieved on an EWD chip via fluorescent signal measurement and two-dimensional magnetic bead concentration. Magnetic bead concentration is controlled with an integrated microelectromagnet, a planar set of half-circle-shaped current-carrying wires embedded in an actuation electrode of an EWD device. This two-dimensional wire structure serves as a microelectromagnet capable of segregating magnetic beads into an area on the order of 10 μm2 with a resulting improvement in Signal-To-Noise Ratio (SNR) of 30 times. Simple device integration ensures that the magnetic bead manipulation and the EWD function can be operated simultaneously without introducing additional steps in the EWD chip fabrication process. Immunological reaction kits were selected in order to ensure the compatibility of target cells, magnetic beads and EWD functions. The magnetic bead choice ensures the binding efficiency and survivability of target cells. The magnetic bead selection and binding mechanism used in this work can be applied to a wide variety of samples with a simple switch of the type of antibody. Sparse cell fluorescent measurements with good SNR are made possible by using fluorescent stains and a method of concentrating cells attached to beads into a small detection area. Theoretical limitation of the entire sparse sample detection system is as low as 1 colony forming unit/mL (CFU/mL).

Keywords: Cell Manipulation; Electrowetting on Dielectric; Fluorescent Detection; Magnetic Beads; Magnetic Beads Control; Sparse Cell Detection

Introduction

Microfluidics technology has been investigated for use in a broad range of biomedical applications [1,2]. In particular, current interest in microfluidic cell analysis has grown significantly in recent years and is driven by several critical platform characteristics, including high speed, fully automated liquid manipulation, flexibility of multiple sensor integration, and reduced usage of reagents [3-6]. Among myriad microfluidic technologies, digital microfluidics based on Electrowetting-On-Dielectric (EWD) technology has the unique advantages of handling small volumes of liquid on reprogrammable liquid pathways with precise control and rapid liquid manipulation [3,7,8]. Accordingly, integration of device technologies that facilitate cell analysis on a digital microfluidics platform harbors the potential for deep impact to a broad range of biomedical applications. Reductions in time for cell detection is essential to process-intensive analysis of complex samples required by many biomedical applications. Once a cell is detected, other important analytical operations such as lysing, Polymerase Chain Reaction (PCR), and sequencing can be conducted, provided cell detection does not overly extend the protocol time. Positive cell detection gives confidence to the researcher that time, reagents, and effort will not be wasted by processing an empty sample, which is often the case.

Rapid detection of target cells in complex samples has its own merit as well. For instance, in septic shock treatment, it is vital to determine the pathogen and provide effective antibiotic treatment, since the survival rate is 58% within 5 hours after

the onset of hypertension [9]. Effective treatment of this grave condition requires rapid detection and identification of circulating pathogens, and current methods based on cell culturing are simply too slow [10,11]. Rapid cell detection, on the other hand, has its own unique sets of challenges [7,12-14]. First, a detection platform needs to be capable to manipulate, analyze, and sense a wide variety of cells at low concentrations. Second, a platform must detect sources of pathogenicity as quickly as possible. Utilizing the rapid liquid manipulation, reprogrammable liquid path and small reagent usage characteristics of digital microfluidics, it is possible to achieve faster target cell detection in a complex sample. This paper introduces a hybrid approach for detecting specific target cells of low concentrations in conjunction with a digital microfluidic platform. We introduce a microelectromagnet integrated with an EWD actuator to concentrate target cells and enhance SNR by a factor of 33.

The general approach as discussed in many publications for detection of sparse cells in a complex sample usually consists of two steps: enrichment and detection [8,10,15-19]. This paper employs a similar strategy to realize sparse cell detection. Enrichment may be assisted by multiple approaches including the use of magnetic micro- or nanoparticles decorated with capture antibodies. The use of small magnetic beads increased the ratio of capture antibodies to magnetic material. Additionally, magnetic bead geometry has been investigated to increase the likelihood of tumor-cell binding with antibodies on the bead structure. After the enrichment stage, the cells were labeled with magnetic particles in order to be manipulated to certain locations where detection was performed [13]. The sparse cell detection device and protocol demonstrated in this paper combines the benefit of a digital microfluidics platform and the sparse cell detection approach.

On-chip cell manipulation is necessary for digital microfluidics to perform cell analytical tasks [7,17,20-22]. A digital microfluidics platform has the potential of integrating multiple biological sensors, which creates possibilities of performing multiple analyses on the same device during the experiment [16,18,23-25]. This leads to the necessity of moving cells to specific locations on the platform. Using droplets to transport and immobilize cells to a detection location is a viable choice provided the detection resolution is greater than or equal to the dimensions of the droplet. However, as the size of a biosensor is reduced, cell manipulation resolution achieved by moving droplets can no longer reliably position the cells to the location of the biosensor. Hence, in order to fulfill the detection requirement of the biosensor, higher resolution cell manipulation techniques must be developed. For current digital microfluidic platforms that typically operate on nanoliter-scale droplets, this implies that cell manipulation needs to happen within a single droplet.

The goal of this paper is to introduce a device that is easily integrated with a digital microfluidic device and an accompanying bead-based approach for detecting sparse target cells. Our approach combines a digital microfluidic platform with high resolution magnetic bead manipulation, and fluorescence microscopy for sparse cell detection. Device operation comprises the following processes: 1) off-chip capture of fluorescently stained cells and extraction from a milliliter volume sample; 2) off-chip cell concentration and re-suspension in microliter volumes suitable for EWD device processing; 3) on-chip bead manipulation to enhance fluorescent signal detection by bead concentration in a small area within a droplet; and 4) fluorescent detection of cells localized within the small area. Intra-droplet magnetic bead manipulation was accomplished with a microelectromagnet that leverages a set of concentric semi-circular current-carrying wire loops embedded in an EWD actuation electrode. Actuation of magnetic beads forces the beads into smaller and smaller wire loops, thereby concentrating target cells and enhancing SNR of fluorescently labeled cells. The SNR of fluorescent measurements is enhanced by concentrating magnetic beads into a reduced sensing area of tens of square microns. This way, the detection limits of our sparse sample detection experiment can be as low as one colony forming unit/mL (1 CFU/mL).

Device Design and Theory

The theory of EWD actuation previously has been reviewed, hence a brief description of the theory of EWD is presented in this section [3,26]. The EWD system consists of top and bottom plates that sandwich a fluid layer. The bottom plate comprises conductive electrodes that are patterned on an insulating substrate and a dielectric layer that is deposited over the electrodes. The top plate is grounded during operation. Both surfaces of top and bottom plates are modified to be hydrophobic. When a voltage is applied to an electrode, the contact angle of the droplet on the dielectric surface is changed. Electric potentials applied between the EWD electrodes and the top plate counter electrode reduce the contact angle of a droplet positioned on an electrode, thus increasing the wetting area of the droplet. Additional details of the operation of the EWD devices used in this study have previously been published [3,7,27].

The manipulation of magnetic beads inside a droplet on a EWD platform is realized by selectively passing current through wires embedded in a control electrode beneath the droplet. The structure was designed based on the Biot-Savart law. The basic structure of the microelectromagnet is a current-carrying wire. Passing current through wires introduces a local, non-uniform magnetic field. This induced magnetic field magnetize superparamagnetic beads in its vicinity. The non-uniformity of the magnetic field inherently possesses a gradient that imparts force that can be used

to manipulate magnetic beads [15,26,28,29]. Thus, if wires run beneath a droplet containing magnetic beads, the magnetic field gradient creates a force that acts on the beads, which are attracted to the location of the peak of the magnetic field. Calculations of the magnetic force created in a parallel current wire system were described in Ref. 3.

In the present work, the parallel current wire structure described in Ref. 3 has been modified to allow two-dimensional magnetic bead manipulation. By patterning the current wires into nested half-circle shapes, it is possible to generate 2D magnetic field gradients from wire currents that can concentrate magnetic beads into a small local area. The basic structure is shown in the (Figure 1). In the figure, the simulated magnetic field is shown when current passes through an arch-shaped wire. The peak field occurs at the top of the arch. This local field optimum attracts magnetic beads in its vicinity to concentrate in that area.

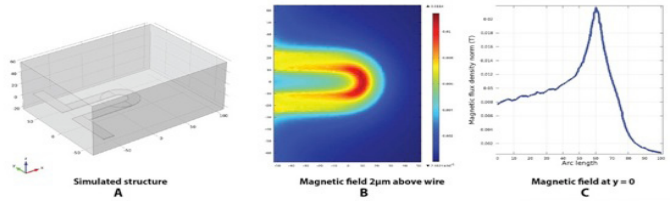

Figure 1: Half-circular wire arch for 2-D magnetic bead concentration. A: Similar to the previous structure, the wire is also used as the basic device for magnetic field generation. B: After current is passed through the wire, a magnetic field is also calculated 2μm above the wire. C: There is clearly a peak in the field at the inner corner of the structure's turn [26].

Sparse Cell Detection System Design

The hybrid approach for extracting cells off-chip and detecting the cells on an EWD platform consisted of two stages as shown in (Figure 2). The first stage was off-chip sample preparation; it included cell binding, washing and volume reduction steps [30]. The original target cell sample of 1 mL volume solution was collected in a 14mL polystyrene tube. Before loading, each cell type was cultured and diluted to the desired concentration. Cells were added into an antibody-enriched solution, where the cells and antibodies were thoroughly mixed and incubated for 15 minutes. Up to three types of cells were used in the initial 1 mL sample: The target cells were *E. Coli* K12, and the noise cells were *Staphylococcus epidermidis* (*S. epi*) and human melanoma cells. The selection of the target cell was determined largely by the ease of handling, availability of an antibody and physical shape to facilitate cell identification in a microscope. LIVE/DEAD™ *Bac*light™ Bacterial Viability kit's fluorescent dye purchased from Thermal Fisher was later added to the sample solution in order to stain the cells in the solution.

The off-chip target cells in the original cell sample were incubated with the added magnetic beads. Mixing and incubation for 15 min ensured the binding between target cells and magnetic beads. Then washing and resuspension in 5 to 10 microliters, depending on protocol, was performed to concentrate the bead-bound target cells so that the volume was suitable for the microfluidic platform [31]. Although the cell concentration was increased at this stage, due to the limited cell count, it was still not possible to confirm the presence of target cells following off-chip sample processing. In addition, no efforts were made to speed the time required for off-chip processing. The gains in cell identification reported here are to determine whether a specific target cell is present before proceeding with time consuming analytical operations such as lysing, Polymerase Chain Reaction (PCR), and sequencing.

The second stage of the protocol was cell concentration on the microfluidics platform for enhanced detection, also shown in (Figure 2). The reduced volume of sample containing only target cells was input into the integrated device with both EWD function as well as the magnetic function. The on-chip detection occurred by concentrating the beads into a small area by the current wire method described in (Figure 1). The entire system approach is illustrated in the (Figure 2), which shows both off-chip and on-chip processes. The first part of the protocol involved off-chip extraction, concentration and volume reduction of target cells, while the second half of the protocol involved dispensing the concentrated sample into multiple smaller droplets. Each droplet was actuated to the detection location, where further target cell concentration was performed prior to detection.

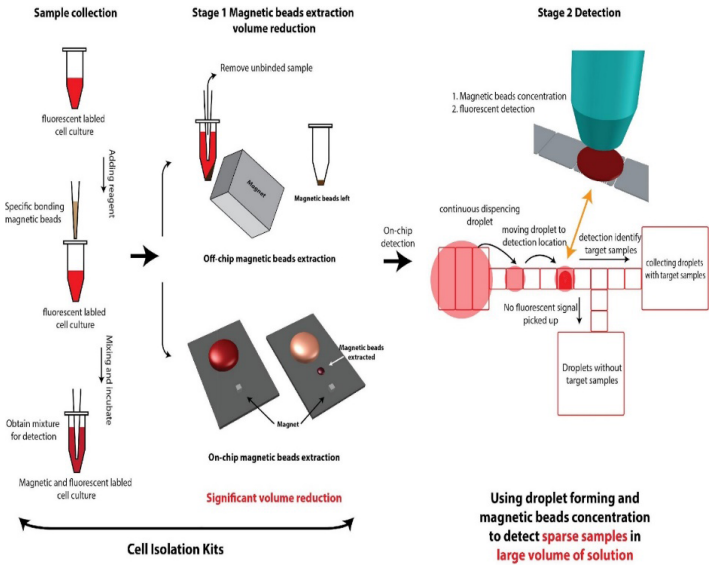

Figure 2: Sparse sample detection approach. Cell isolation, bead extraction and bead resuspension are done off-chip. The resuspended bead sample is loaded onto the microfluidic chip for cell detection.

Biological Sample Labeling and Washing Function Design

Cell capture studies initially used Dynabead M-270 streptavidin-coated magnetic beads. However, these beads could not be fully actuated in droplets on our EWD devices, since a significant number of beads would become attached to the hydrophobic insulator over the actuation electrodes [32]. It was unclear whether the problem was due to surface charge on the beads attracted to the CYTOP layer on chip or if there was binding between the hydrophobic beads and the hydrophobic CYTOP [33,34]. On the other hand, since carboxylic acid is hydrophilic, it was determined that full EWD actuation was possible with Dynabead M-270, carboxylic acid-coated magnetic beads. This bead choice also was made since the selected antibodies could easily bind to the beads' surface without an additional binding mechanism. The binding between the antibody and carboxylic acid coating is a covalent bond, which is strong enough for subsequent magnetic bead manipulation during cell capture and washing. The Dynabead M-270 beads also had high magnetic content, which made the manipulation of target cells easier on chip. The antibody of choice for carboxylic acid functionalized beads was the *E. coli* antibody [Anti-E. coli antibody (ab25823) purchased from Abcam], which can be used to bind with *E. Coli* K12, O157 and others.

By studying the cell yield during cell capture, washing and volume reduction, it was determined that 87% of the target cells were damaged or killed during the magnetic bead extraction steps in (Figure 3) when using the carboxylic acid functionalized Dynabead M-270 beads. This loss likely was due to the large diameter and high magnetic content of the Dynabead M-270 beads. However, using the much smaller EasySep magnetic beads with Dextran coating allowed a high survival rate (>93%) for target cells. The protocol for target cell capture using EasySep magnetic beads was based on the protocol supplied by STEMCELL Technologies [35]. The binding between target cells and EasySep magnetic beads required the steps listed below:

- Prepare cell suspension in Phosphate Buffered Saline (PBS) with 2% Fetal Bovine Serum (FBS). Cells need to be placed in a 5 mL (12 x 75 mm) polystyrene tube to properly fit into the custom-made magnet. The tube of choice is Falcon™ 5 mL Polystyrene Round-Bottom Tubes (Becton Dickinson, Catalog #352058).
- Add FITC-conjugated antibody* at a final concentration of 0.3 - 3.0 µg/mL. Mix well and incubate at room temperature for 10 minutes.
- Add EasySep® FITC Selection Cocktail at 100 µL/mL cells (e.g. for 2 mL of cells, add 200µL of cocktail). Mix well and incubate at room temperature for 15 minutes.
- Mix Magnetic Nanoparticles to ensure that they are in a uniform suspension by vigorously pipetting more than 5 times. Add the nanoparticles at 50 µL/mL cells (e.g. for 2 mL of cells, add 100 µL of nanoparticles). Mix well and incubate at room temperature for 10 minutes.
- Bring the cell suspension to a total volume of 2.5 mL by adding Phosphate Buffered Saline (PBS) with 2% Fetal Bovine Serum (FBS). Mix the cells in the tube by gently pipetting up and down 2 - 3 times. Place the tube (without cap) into the magnet. Set aside for 5 minutes.

At this stage, the target cells in the complex sample were bound to the magnetic beads and the other cell types in the sample that were not of interest were not bonded. Then, fluorescent labeling gave the target cells a detectable marker. The easiest labeling technique, staining, was selected to give a fluorescent signal to the target cells. The SYTO 9 stain [36] was used to stain the live target cells and to provide green fluorescent light (480nm/500nm) for detection, while presidium iodide [37] was used to stain non-living target cells with a red emission spectrum (530nm/620nm). The protocol [38] for staining the cells only took 10 minutes, and the only operation required was to mix the stain with sample solution thoroughly.

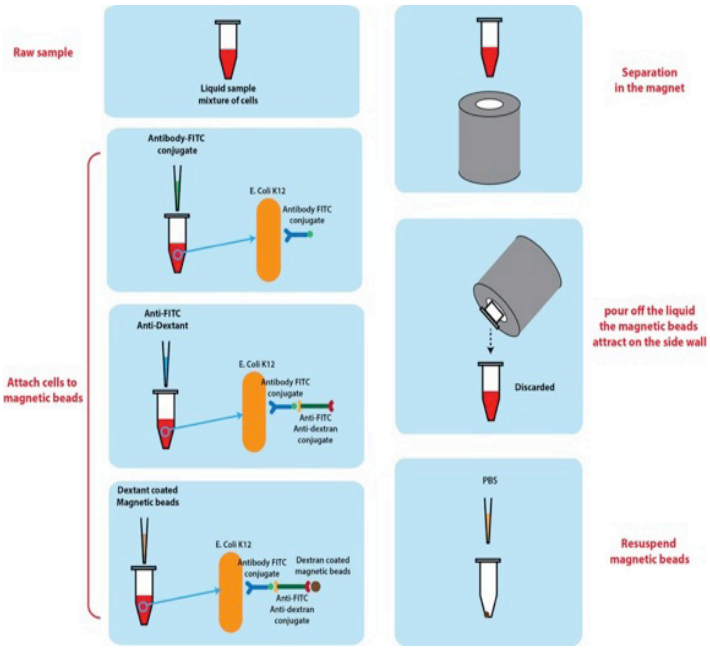

Figure 3: Magnetic beads binding mechanism with target cells.

The detailed protocol is shown in (Figure 3). The washing and re-suspending protocol required the steps below [35]:

- Pick up the magnet, and in one continuous motion invert the magnet and tube, pouring off the supernatant fraction. The magnetically labeled cells will remain inside the tube, held by

the magnetic field of the external magnet. Leave the magnet and tube inverted for 2 - 3 seconds, then return to upright position. Do not shake or blot off any drops that may remain hanging from the mouth of the tube.

- Remove the tube from the magnet and add 2.5 mL Phosphate Buffered Saline (PBS) with 2% Fetal Bovine Serum (FBS) medium. Mix the cell suspension by gently pipetting up and down 2 - 3 times. Place the tube back in the magnet and set aside for 5 minutes.
- Repeat previous two steps for a total of 3 x 5-minute separations in the magnet. Remove the tube from the magnet and re-suspend cells in an appropriate amount of desired medium. The positively selected cells are now ready for use
- After washing the target cells and magnetic beads, they were re-suspended in 20μL of DI water, and the solution was pipetted into the EWD device reservoirs for observation. A Zeiss Axio imager was used to observe the resulting solution, and also target cell washing was assessed using the microscope.

Integrated Device Design

An EWD chip was designed for the purposes of investigating the Two-Dimensional (2D) concentration of cells using magnetic beads in a micorelectromagnet, described above in (Figure 1). This hybrid device was used to demonstrate a sparse sample detection experiment enabled by the 2D concentration function of micorelectromagnet interacting with superparamagnetic beads immunologically bound to target cells. Three design requirements were used as design guidelines for the micorelectromagnet structure. First, the device should be able to simultaneously perform electro wetting to move droplets as well as magnetic bead manipulation. Second, the manipulation of magnetic beads should occur within the droplet, and both electro wetting and magnetic bead manipulation should function without interfering with each other. Finally, the same metal layer that comprises the EWD electrodes should form the micorelectromagnet device. This requirement obviates the need for additional fabrication steps relative to a conventional EWD device.

As shown in (Figure 4), the layout of the integrated EWD-micorelectromagnet differs from a standard EWD electrode. The integrated device comprises an EWD electrode with a modified geometry that accommodates the concentric wire loops that comprise the micorelectromagnet, all of which are deposited in the same metal layer. Since the device in (Figure 4) is targeted towards sparse sample detection, target cell concentration in a small area is required. In this second device, 2D concentration of magnetic beads is required, which means the device concentrates all the target cells into a small location where the optical detection takes place.

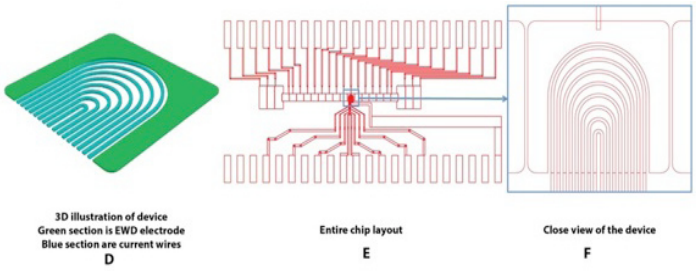

Figure 4: Layout of the 2-D magnetic manipulation chip. D: The 3D figure showing the device has both current wires and EWD electrode. E: layout of the entire chip used to verify the device's function. F: An enlarged figure showing the magnetic concentration device.

As shown in (Figure 4), the basic building block of the micorelectromagnet is a semi-circlular wire loop. A COMSOL Multiphysics simulation was developed to predict the magnetic field produced by the micorelectromagnet. The simulation shows that the uneven distribution of current density in the wire creates a single peak in magnetic field strength. The presence of multiple concentric loops with decreasing radius enables magnetic beads to be moved from outer wires to inner-most wire by sequentially switching current on in subsequent wire loops. During droplet operation, the micorelectromagnet wires were also energized with voltage to facilitate the droplet actuation. By using the same layer structure as all the other devices described in the paper, the single-pattern fabrication process for simple EWD device is preserved.

Device Fabrication

The top plate serves several key functions: it provides a viewing window and a hydrophobic surface for EWD droplet manipulation; a ground plane for electrowetting; and last, a fluidic seal to prevent evaporation of liquid. To accomplish these tasks, the top plate is implemented as a 0.5 mm thick acrylic slab. Top plates were formed by laser cutting acrylic sheets into rectangular geometries that assemble with EWD bottom plates. After the top plates were cut, one side of the top plate was sputter coated with an 80 nm thick film of Indium Tin Oxide (ITO). This layer is grounded during experiments for electrowetting. Lastly, a thin layer of CYTOP was applied over the ITO ground plane by spinning. After Baking at 100˚C for 5 min, the top plate is complete. The gasket layer is simply a layer of adhesive material that bonds the top plate with the bottom plate with a certain height. As such, this layer defines the thickness of liquid channels for the device. The fabrication of the gasket layer is similar to the fabrication of the top plate. The gasket layer is made from Secureseal® sheets from Grace Bio-labs. An entire sheet of Secureseal® is placed in the laser cutter and the multiple gasket layers are cut into shape. By removing the top and bottom protective membranes on the Secureseal® sheets the gasket

layer was then placed between the top plate and bottom plate, thus creating a sealed chamber.

The bottom plate is based on a 450 µm silicon wafer with 1 µm thick thermal oxide on top. The thermal oxide was used to promote adhesion between the wafer and the conductive layer. The wafer with thermal oxide was purchased and cleaned prior to subsequent processing. The conductive, device layer was deposited above the 1 µm thick thermal oxide. The material of choice was a Ti/Cu stack. The thickness of the Ti layer is only 10 nm while the thickness of the Cu layer was 1 µm. The thickness of Cu was chosen to handle the high current densities ($10^6 A/cm^2$) required for magnetic bead control. The Ti serves as an adhesion layer between the oxide and Cu. The metal layer was first deposited as a blanket layer onto the wafer and then S1813 photoresist was spun onto the wafer and patterned. After developing, the metal layer was patterned with a wet etch step.

Parylene-C, a common electrowetting dielectric, was then deposited above the metal layer. This insulator layer was vacuum deposited over the conductive layer at a thickness of 2 µm and with simple shadow masking over electrode areas intended for external contact. The 2 µm thickness was selected to promote device reliability while allowing for sufficient magnetic force when the microelectromagnet was activated. After the insulator layer is formed, CYTOP is spun onto the device at thickness of 80 nm and baked to complete the bottom plate fabrication.

Experiments

The capability of basic magnetic bead manipulation and SNR enhancement with current-carrying wires integrated on an EWD platform was previously reported. However, the experiments in this work demonstrate the utility of the microelectromagnet device to operate on sparsely concentrated cells with minimal impact to cell viability [18]. In order to demonstrate cell capture, detection, and SNR enhancement, experiments were performed to verify 1) that target cells could be separated from large-volume (1 mL) sample solutions, and 2) that the separation of target cells from a complex sample solution containing noise cells, and 3) to demonstrate the on-chip concentration of target cells into a localized area to enhance fluorescent detection.

Captured Biological Sample Manipulation

The separation and manipulation of the captured biological sample consisted of three steps. The first step was to selectively bind the target cells with magnetic beads in a complex environment; the second step was to segregate the target cells from the rest of the sample, and the third step was to wash the target cells so that only the cells of interest were placed onto the chip. The fluorescent cells attached to magnetic beads were then manipulated using the microelectromagnet device integrated with the EWD platform. Fluorescence microscopy was used to observe the concentration of the magnetic beads. The cells used to simulate the complex environment included *Staphylococcus epidermidis* (*S. epi*) and human melanoma cells. The target cell was *E. coli* K12. It is noted that the physical shape and size of *E. coli* K12 is significantly different from the two noise cells of selection.

The target cells together with noise cells are all shown in the (Figure 5) above. The *E. coli* K12 cell sample is cultured by placing 1 mL of cell stock solution in 10 mL of LB broth in a 14-mL tube, and the tube was placed in a tumbler for 20 hours at 30˚C. After 20 hours, the culture was diluted to a cell concentration of 10^7cells/mL. *S. epi* cells were cultured using the same procedure as *E. coli* K12 cells and they were added to the sample solution at a specific concentration. The human melanoma cells were added to the sample directly from stock solution purchased from the Cell Culture Facility at Duke University. The final concentration of each kind of cell is 10^7 cells/mL in the complex sample solution. Fluorescent dye was added to the complex solution so that all three kinds of cells were visible under the fluorescent microscope.

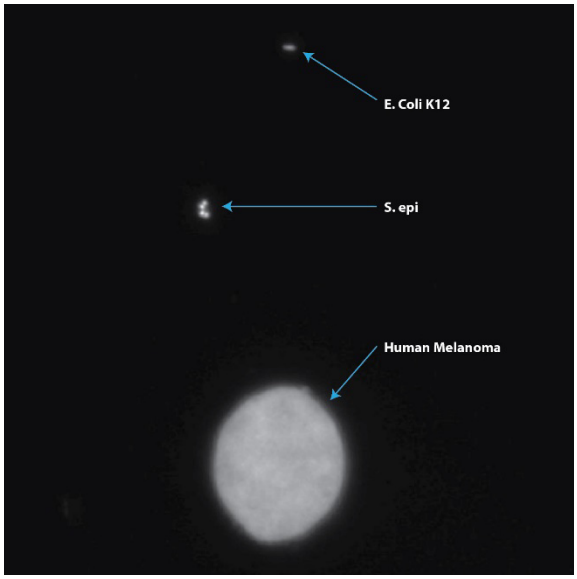

Figure 5: Target cells and noise cells.

EWD Testing and Optical Microscopy

The setup used for the experiment required an imaging system, EWD controller, and magnetic bead manipulation control setup. The imaging system was intended for observation of both bright light as well as fluorescent signals. The fluorescent microscope used in the experiment was the Zeiss Axio Imager. The two fluorescent dyes used in the experiment were FITC fluorescent dye and Cy5 fluorescent dye. As a result, the microscope accommodated two sets of filters. For FITC fluorescent dye, the excitation and emission wavelength was 450 nm-490 nm/550 nm-

550 nm respectively. For Cy5 fluorescent dye, the excitation and emission wavelength was 620 nm-650 nm/660 nm-720 nm. The lens choice included 5x, 10x, 20x and 40x magnification, and the microscope had sufficient working space for the experiments at 5x magnification. The Zeiss Axio Imager was equipped with a CCD camera, and leveraged Meta Morph software for raw data capture and image analysis.

The EWD voltage used in controlling the droplets was an AC signal of sufficient voltage magnitude (40V) to change the surface energy of the device. To achieve this voltage, the combination of waveform generator and amplifier were used to first generate the AC sinusoidal signal at a specific frequency (10 - 1000Hz) and then the signal was fed into the amplifier to reach the required voltages. The controller was designed to pass EWD voltages to different electrodes for droplet actuation. Due to the high voltage magnitude used in EWD experiments, an optical relay array was used to drive 32 electrodes on the EWD device. As previously outlined above, magnetic beads were manipulated by the magnetic field generated from current passing through the microelectromagnet. A 5A power supply was used to supply the high current used in to generate magnetic fields sufficient for bead manipulation. Optical relays were also used to control the current. The optical relays used were capable of supplying current up to 1 A, and the switching time for the current was 10 ms. The highest current used in the experiment was 300 mA.

Sparse Sample Detection

The sparse sample detection experiment combined the 2D magnetic bead concentration technique and the bead washing protocol designed to preserve the maximum concentration of target cells extracted from a complex sample solution. Sample detection was evaluated in a series of three preliminary experiments that led to a demonstration of sparse target cell detection. First, we tested the 2D magnetic bead manipulation function using the microelectromagnet. This objective of this experiment was to verify the capability of the device and is also the foundation for the subsequent steps. Second, we evaluated the bead binding and washing steps for rejection of all the noise cells in the complex sample while maintaining high viability of the target cells. Third, we quantified detection sensitivity in terms of lowest target cell concentration explored optimum stoichiometry of magnetic beads and target cells.

Finally, a demonstration of sparse cell detection was performed with target cell concentrations from 10^4 - 10^5 cells/mL. Prior to detection, the cells went through binding, fluorescent staining and washing steps. After separation of target cells, the magnetic beads with target cells attached were resuspended in the reduced amount of liquid (20 µL). The liquid was then pipetted into the reservoir of an EWD test device. Fluorescence detection was then conducted on each droplet that was dispensed from the reservoir and moved onto the detection electrode. The culture of the target cells was prepared the same way as in the previous experiment. The *E. coli* K12 cells, *S. epi* cells and human melanoma cells were cultured individually then mixed to form the complex sample. The magnetic bead choice in the previous experiments introduced significant cell loss after the washing step. Sparse cell detection required that the cell binding mechanism and the washing function to be performed with high viability of the target cells, while rejecting as many of the noise cells as possible.

The magnetic bead choice in this experiment was the Easy Sep magnetic particles. These particular magnetic particles are much smaller in size than the Dynabeads M-270, and are synthesized with a Dextran surface coating. To achieve magnetic bead concentration on the magnetic microelectromagnet device, current was sequentially switched from the outer loops with larger diameters to the inner wire loops with smaller diameter. Concentration was completed when all the magnetic beads with attached target cells were located in a small area in the center of the circular area of the inner most wire. (Figure 6) illustrates the current switching pattern used. The current magnitude used to concentrate cells was 200 mA. The switching time between each wire was 3 secs, to maximize the number of magnetic beads with target cells actuated from one wire to the next.

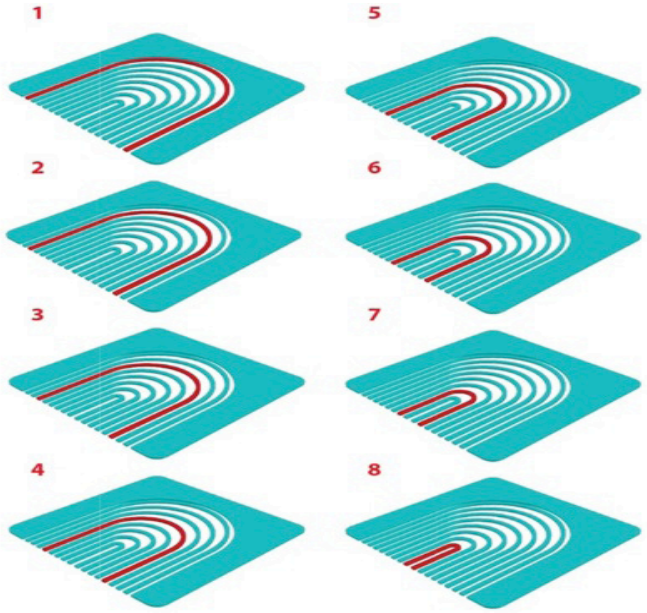

Figure 6: Current wire switching pattern for 2-D cell-bead concentration.

Results

Initially an experiment was aimed at verifying the

functionality of 2D bead concentration. To test this functionality, cells were not included in the experiment, since target cells could be simulated by fluorescently-labeled magnetic particles. The fluorescent magnetic particles used in this experiment were the Encapsulated Magnetic Polymer beads (Bangs Laboratory). Concentration enhancement was evaluated by comparing integrated fluorescence signal intensity in a 10 μm^2 encompassing the innermost loop of the magnetic microelectromagnet before and after the concentration step. (Figure 7) shows fluorescence micrographs of the microelectromagnet device before and after concentration enhancement.

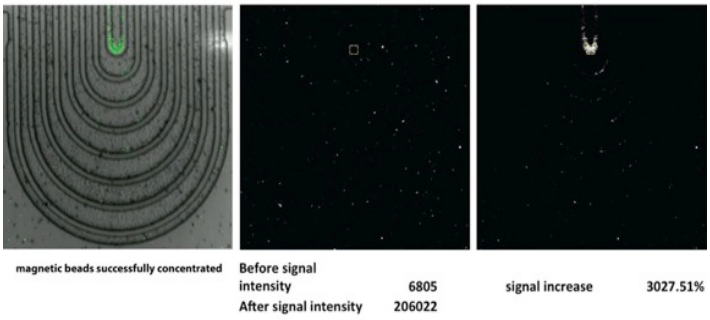

Figure 7: 2-D concentration with fluorescently labeled magnetic particles.

It can be seen in (Figure 7) that the magnetic beads were successfully collected at the center of the microelectromagnet, as shown in the left most image, from a uniformly dispersed sample shown in the middle image. This result indicates that the microelectromagnet was able to manipulate magnetic beads and focus them into a small area, effectively enhancing their concentration. Comparison of the bead concentration in the square region shown in the figure to the same region in (Figure 7c) revealed that the SNR of the fluorescence signal attributed to the magnetic beads increased by a factor of about 30.

After confirming the functionality of the 2D concentration enhancement method and showing that the actual SNR could be improved, the microelectromagnet device was tested with actual magnetic beads used in the washing protocol. The EasySep Dextran coated magnetic beads purchased from Stemcell in the final protocol were tested with the microelectromagnet device. As shown in (Figure 8), magnetic beads were visible under the bright field microscope. The yellow arrows in (Figure 8) highlight the presence of the EasySep magnetic beads. Concentration enhancement was confirmed by the presence of magnetic beads, which were identified as a dark area surrounding wire loops in the microelectromagnet device.

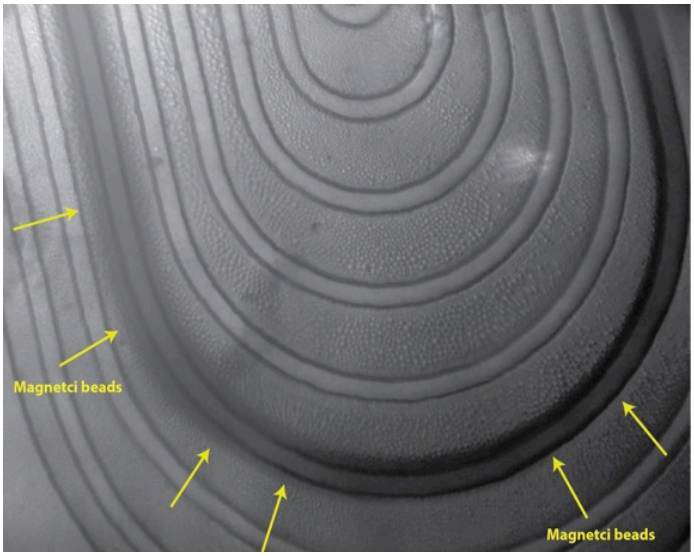

Figure 8: EasySep magnetic beads in 2D current-wire electrode.

After verifying magnetic concentration enhancement in the microelectromagnet device, the retention rate of target cells following the washing step was quantified. The washing step should ideally remove all noise cells while maintaining the maximum amount of target cells. The retention rate is calculated by dividing the cell concentration after washing to the cell concentration before washing. Following the protocol for binding cells to EasySep beads [35], the number of cells bound in solution prior to washing was counted by fluorescence microscopy and Image J software. The magnetic bead solution was prepared by diluting 10 µL of stock solution containing target cells (1.3×10^5 cells/mL) into 2.5 mL of DI water in a 12 mL tube. After magnetic separation, the supernatant was poured into another tube and the residual beads with attached cells were resuspended in 2.5 mL of DI water. Fluorescence microscopy again was used to count the number of resuspended beads/cells and the number of beads/cells in the supernatant. (Table 1) shows the results of three independent washing steps, where the average retention efficiency was about 93.7%

During the washing steps with EasySep beads, only minor levels of cell loss occurred, as evidenced by comparing the relatively small number of target cells found in supernatant volumes. Cell loss is primarily due to the unbounded cells in the starting solution, which were decanted with the supernatant. Thus, EasySep magnetic beads with Dextran coating offers high cell retention rates for *E. coli* K12 target cells, and therefore are appropriate for use in the sparse sample detection application.

	Number of Cells Attached to breads	Number of cells Supernatant	Survival Efficiency
1	614	45	
2	633	36	
3	693	50	
Average	646.78	43.67	93.68%

Table 1: Cell number in both washed sample and supernatant.

The conclusion drawn thus far is that the EasySep magnetic beads with bound target cells can be manipulated on an EWD device using the proposed microelectromagnet device, and cell/bead washing can be accomplished with high cell retention (> 93%) of the target cells. The third experiment was conducted in order to determine if a small concentration of magnetic beads could be used to capture target cells in a low concentration cell sample. Due to the low concentrations of both magnetic beads and target cells, small amounts of magnetic beads may not be sufficient to capture sparse cells in a diluted sample.

A total of four target cell solutions were prepared from a target cell stock solution with concentration of $1.3x10^9$ cells/mL. For each of the two target cell concentrations, two diluted sample aliquots were diluted with PBS to concentrations used in the experiment. The two concentrations of target cells are $1.3x10^5$ cells/mL and $1.3x10^2$ cells/mL, respectively. These samples were prepared by diluting the stock solution in PBS. By changing the amount of stock solution, the concentration of target cells in the solution was controlled. After the magnetic beads were isolated, pelleted and the supernatant poured off, decanted, 2.5 mL of LB broth was added back to the 12 mL tube and mixed with magnetic beads with target cells attached. The solutions were cultured at 30°C for 20 hours to confirm if there were the any captured cells present. After 20 hr. of growth, if there were any cells captured by the magnetic beads, the solution would become opaque and could be easily identified. The result showed target cell growth in every tube after 20 hr. This was a confirmation that, even with 130 cells/mL of target cells combined with lowest the concentration of magnetic beads, the protocol can still capture target cells in the solution.

The last experiment used all the information and methods developed previously. The experiment started with target cells and noise cells in the same solution, and the concentration of target cells was $1.3x10^5$/mL. After cell binding, washing and re-suspension, the sample solution was loaded into the reservoir on the EWD chip for dispensing. A droplet was dispensed from the reservoir and actuated along the string of electrodes to the microelectromagnet device, where magnetic bead concentration was performed. When the concentration of target cells is low, there is chance that each 120 nL droplet dispensed on chip contains a number of cells less than an average number. By dividing the total number of cells with the total number of droplets, the average number of cells in each 120 nl droplet was calculated to be around 50. Accordingly, the detection limit of the microscope is very important to ensure the detection of very low numbers of target cells. The fluorescence micrograph included in (Figure 9) shows the result of the concentration enhancement of target cells inside of a single 120 nL droplet.

To determine the Limit of Detection (LOD) using the image captured, the equation shown below was used [39]:

$$LOD = \mu_{blank} + 3\sigma_{blank}$$

where μ_{blank} and σ_{blank} refer to the mean and standard deviation of the signal of the background.

In order to investigate if it is possible to detect a single target cell in the detection area, a detection area of the same size as described before was used, which is 30 pixels by 30 pixels.

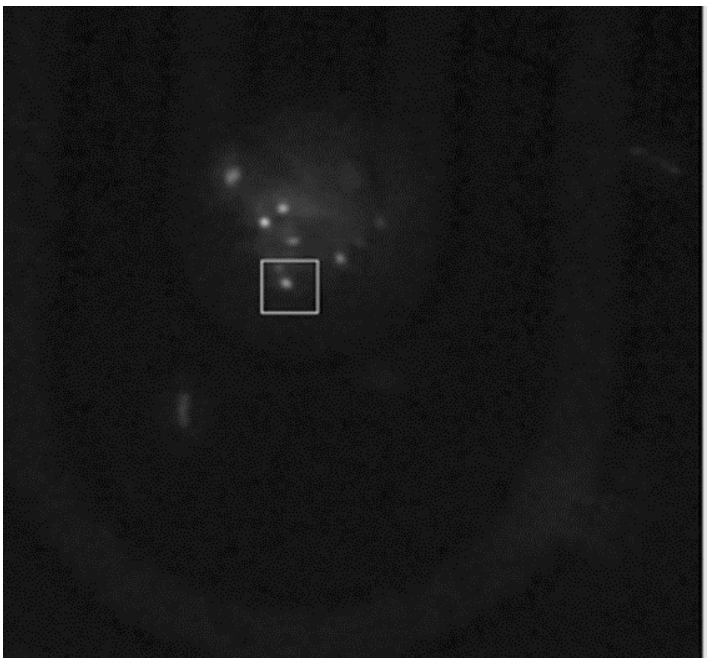

Figure 9: Detection area only contains one cell.

Using the captured image shown in (Figure 9) and by moving the detection area, we were able to achieve having only one target cell in the detection area. In this case, the average signal intensity of the detection area with target cell inside was 563.451. The standard deviation of detection area without target cell was 3.557 and the average signal was 496. Using Eq. 4, we can calculate that the detection limit of the system is 506. The average signal in the detection area having the target cell is 563.451, which is larger than the detection limit. Hence we can conclude that with 20 ms

of integration time, the system is also capable of detecting single target cells in a droplet.

The same detection experiment was conducted several times and in each case, the detection limit was always lower than the average signal in the detection area. Hence, we can conclude that the LOD of the CCD sensor satisfies conditions needed to identify single target cells in one droplet. Given the detection system's LOD, we can proceed to calculate the minimum target cell concentration in 1 mL of initial sample, which could be detected with the proposed protocol. Considering the total volume of liquid that needs to be loaded onto an EWD chip is 20 μL and each droplet has volume of 120 nL, there would need to be 167 droplets measured. Given one of the 167 droplets generates a positive detection result, we can conclude that if 1 target cell can be detected in 20μL of resuspended solution, then for a 100% efficient washing and re-suspension process, it would be possible to capture and detect 1 cell/mL (1 CFU/mL). This work has demonstrated that while the entire system has a demonstrated capability of detecting target cells with concentrations as low as 130 CFU/mL a feasible theoretical limit is 1 CFU/mL.

Conclusion and Discussion

The results of this study demonstrate the potential for detecting whether sparse target pathogen cells exist in milliliter solution samples. However, the requirement to detect trace, quantifiable amounts of pathogens in large-volume biomedical samples requires more advanced techniques, such as DNA preparation techniques using modern technologies to facilitate DNA isolation, purification, and analysis by quantitative PCR (qPCR). Nevertheless, the target cell extraction protocols used in the current work can be useful in establishing initially whether considerable time and effort should be expended in quantitative analysis. The target cell detection method described here may be the first step in pathogen identification, and may save both time and reagents in identifying whether the target sample is present at all. The capture and washing protocols are closely related to the magnetic beads of choice. An EWD chip capable of concentrating target cells in two dimensions was designed. An optical detection system was also designed to detect fluorescent signals generated from target cells after concentration. The capability of the detection system was characterized during the experiments.

The experiments verified the functionality of the 2D microelectromagnet bead concentration device. The device used concentric semi-circular wire loops to concentrate target cells attached to magnetic beads into a small detection area. To test this device, fluorescently labeled magnetic beads were used and tested on the 2D microelectromagnet. Based on experimental result, the device can be applied to concentrate target cells using magnetic beads as carriers. The compatibility of EasySep magnetic beads and on-chip 2D bead concentration was also evaluated. Magnetic beads chosen were based on size and whether the bead had a biologically sample friendly dextran surface coating. These two factors were chosen specifically to increase the retention rate of target cells during the washing step. After examining the functionality of the microelectromagnet to actuate magnetic beads, the binding of the magnetic beads to target cells was evaluated to ensure high retention rate of target cells during washing steps. The binding mechanism used in this experiment was the FITC conjugate method. The binding mechanism included an antibody-FITC conjugate, anti-FITC anti-dextran conjugate, and the dextran coated magnetic particles. The binding mechanism revealed that above 93% of the target cells could be captured by magnetic beads. This result provides confidence that appropriate magnetic bead choice and proper binding mechanism can be applied to the sparse biological sample detection application.

Another concern was the concentration of magnetic beads required to run this experiment. The reason to consider this was due to the limitation on the amount of liquid that can be input into the microfluidics system. More magnetic beads require more liquid during the re-suspending step, and hence impose an additional requirement on the system. As a result, an experiment was designed to find the lowest concentration of magnetic beads that could be used to capture and wash target cells. It was shown that 5 μL of magnetic beads was sufficient to separate target cells at $1.3x10^2$ cells/mL concentration. Based on this result, the amount of liquid that will be processed by the system can be determined. During the experiment, 5 μL of magnetic beads required 20 μL of DI water for the resuspension step.

After the device functionality was verified and the magnetic beads were thoroughly tested, a comprehensive experiment was conducted that integrated all the building blocks discussed so far. By starting with low concentrations of target cells, the experiment involved washing, on-chip magnetic concentration and detection. The target cells were captured and washed in a tube using a ring-shaped permanent magnet. The re-suspended sample was then introduced onto the EWD chip. Droplets containing magnetic beads and target cells were dispensed and actuated onto the integrated device. After bead concentration enhancement in the microelectromagnet, a fluorescence microscope was used to detect the presence of target cells. Based on the analysis of fluorescence signals from target cells and background noise statistics, the detection limitation of the optical detection method was found to be as low as one target cell per droplet. As previously discussed the possibility of capturing target cells during capture and washing steps is 93%, and thus the possibility of detecting a target cell concentration of 1 CFU/mL is 93% using the protocol described herein. While this is a theoretical detection limit, the experiment was only able to confirm that a target cell concentration of 130

CFU/mL can be detected. At lower concentrations, the experiment would be impractical to conduct.

Acknowledgement

This work was supported in part by the National Science Foundation under grant NSF-CNS-11-35853.

References

1. Zhu Z, Zhang W, Leng X, Zhang M, Guan Z, Lu J, et al. (2012) Highly sensitive and quantitative detection of rare pathogens through agarose droplet microfluidic emulsion PCR at the single-cell level. Lab Chip 12: 3907-3913.
2. Duncombe TA, Tentori AM, Herr AE (2015) Microfluidics: reframing biological enquiry. Nat Rev Mol Cell Biol 16: 554-567.
3. Fair RB (2007) Digital microfluidics: is a true lab-on-a-chip possible? Microfluid Nanofluid 3: 245-281.
4. Teranishi N, Kohono A, Ishihara Y, Oda E, Arai K (19821) No image lag photodiode structure in the interline CCD image sensor. In: 1982 International Electron Devices Meeting. Pg No: 324-327.
5. Song JH, Evans R, Lin YY, Hsu BN, Fair RB (2008) A scaling model for electrowetting-on-dielectric microfluidic actuators. Microfluidics and Nanofluidics 7: 75-89.
6. Dunlop DJ (1973) Superparamagnetic and single-domain threshold sizes in magnetite. Journal of Geophysical Research 78: 1780-1793.
7. Fair RB, Khlystov A, Tailor TD, Ivanov V, Evans RD, et al. (2007) Chemical and Biological Applications of Digital-Microfluidic Devices. Design & Test of Computers IEEE 24: 10-24.
8. Malic L, Veres T, MaryamTabrizian (2008) Dynamically configurable digital microfluidic-based surface plasmon resonance imaging biochip for DNA hybridization detection. Lab Chip.
9. Molnar L, Berhes M, Papp L, Nemeth N, Fulesdi B (2015) Cerebral autoregulation testing in a porcine model of intravenously administrated *E. coli* induced fulminant sepsis. Critical Care 19: P1.
10. Howell MD, Davis AM (2017) Management of sepsis and septic shock. JAMA 317: 847-848.
11. Martin GS (2012) Sepsis, severe sepsis and septic shock: changes in incidence, pathogens and outcomes. Expert Rev Anti Infect Ther 10: 701-706.
12. Brouzes E, Medkova M, Savenelli N, Marran D, Twardowski M, et al. (2009) Droplet microfluidic technology for single-cell high-throughput screening. Proc Natl Acad Sci U S A 106: 4195-2000.
13. Arya SK, Lim B, Rahman AR (2013) Enrichment, detection and clinical significance of circulating tumor cells. Lab Chip 13: 1995-2027.
14. Rival A, Jary D, Delattre C, Fouillet Y, Castellan G, et al. (2014) An EWOD-based microfluidic chip for single-cell isolation, mRNA purification and subsequent multiplex qPCR. Lab Chip 14: 3739-3749.
15. Kim H, Bartsch MS, Renzi RF, He J, Van de Vreugde JL, et al. (2011) Automated digital microfluidic sample preparation for next-generation DNA sequencing. J Lab Autom 16: 405-414.
16. Lazcka O, Campo FJD, Muñoz FX (2007) Pathogen detection: A perspective of traditional methods and biosensors. Biosensors and Bioelectronics 22: 1205-1217.
17. Lee H, Liu Y, Ham D, Westervelt RM (2007) Integrated cell manipulation system--CMOS/microfluidic hybrid. Lab Chip 7: 331-337.
18. Liao KC, Chiu HS, Fan SY, Tseng YD, Lu PH (2016) Percutaneous fiber-optic biosensor for immediate evaluation of chemotherapy efficacy in vivo (part I): Strategy of assay design for monitoring non-homogeneously distributed biomarkers. Sensors and Actuators B: Chemical 222: 544-550.
19. Ma H, Wallbank RWR, Chaji R, Li J, Suzuki Y, et al. (2013) An impedance-based integrated biosensor for suspended DNA characterization. Scientific Reports 3: 2730.
20. Shields CWT, Reyes CD, Lopez GP (2015) Microfluidic cell sorting: a review of the advances in the separation of cells from debulking to rare cell isolation. Lab Chip 15: 1230-1249.
21. Chen Y, Li P, Huang PH, Xie Y, Mai JD, et al. (2014) Rare cell isolation and analysis in microfluidics. Lab Chip 14: 626-645.
22. Zborowski M, Chalmers JJ, (2011) Rare cell separation and analysis by magnetic sorting. Anal Chem 83: 8050-8056.
23. Ohk SH, Bhunia AK (2013) Multiplex fiber optic biosensor for detection of Listeria monocytogenes. *Escherichia coli* O157: H7 and Salmonella enterica from ready-to-eat meat samples. Food microbiology 33: 166-171.
24. Velusamy V, Arshak K, Korostynska O, Oliwa K, Adley C (2010) An overview of foodborne pathogen detection: In the perspective of biosensors. Biotechnology Advances 28: 232-254.
25. Chen Q, Lin J, Gan C, Wang Y, Wang D, et al. (2015) A sensitive impedance biosensor based on immunomagnetic separation and urease catalysis for rapid detection of Listeria monocytogenes using an immobilization-free interdigitated array microelectrode. Biosensors and Bioelectronics 74: 504-511.
26. Chen L, Fair RB (2015) Digital microfluidics chip with integrated intra-droplet magnetic bead manipulation. Microfluidics and Nanofluidics 19: 1349-1361.
27. Chen L, Madison A, Fair RB (2014) Intra-droplet magnetic bead manipulation on a digital microfluidic chip. presented at the MicroTAS 2014, San Antonio 2014.
28. Wang Y, Zhao Y, Cho SK (2007) Efficient in-droplet separation of magnetic particles for digital microfluidics. Journal of Micromechanics and Microengineering 17: 2148-2156.
29. Zhang Y, Wang TH (2013) Full-range magnetic manipulation of droplets via surface energy traps enables complex bioassays. Adv Mater 25: 2903-2908.
30. Grant IS, Phillips WR (2008) Electromagnetism (2nd Edition): Manchester Physics, John Wiley & Sons.
31. DS Jones. (2013) The theory of electromagnetism: Elsevier 2013.
32. He J, Huang M, Wang D, Zhang Z, Li G (2014) Magnetic separation techniques in sample preparation for biological analysis: A review. J Pharm Biomed Anal 101: 84-101.

33. Gretch DR, Suter M, Stinski MF (1987) The use of biotinylated monoclonal antibodies and streptavidin affinity chromatography to isolate herpesvirus hydrophobic proteins or glycoproteins. Analytical biochemistry 163: 270-277.

34. Young T, Abel R, Kim B, Berne BJ, Friesner RA (2007) Motifs for molecular recognition exploiting hydrophobic enclosure in protein-ligand binding. Proceedings of the National Academy of Sciences 104: 808-813.

35. Stemcel. Product Information Sheet for Stemcell FITC Selection Kit. ed.

36. Fisher T (2016) SYTO® 9 Green Fluorescent Nucleic Acid Stain 2016.

37. Fisher T (2016) Propidium Iodide 2016.

38. Fisher T (2016) LIVE/DEAD® BacLight™ Bacterial Viability Kit, for microscopy 2016.

39. Armbruster DA, Pry T (2008) Limit of Blank, Limit of Detection and Limit of Quantitation. The Clinical Biochemist Reviews 29: S49-S52.